Molecular Pharmacology Fast Forward. Published on February 2, 2017 as DOI: 10.1124/mol.116.106633
This article has not been copyedited and formatted. The final version may differ from this version.

MOL #106633

Sequence-specific regulation of endocytic lifetimes modulates arrestin-mediated signaling at the μ opioid receptor

Zara Y. Weinberg, Amanda S. Zajac, Tiffany Phan, Daniel J. Shiwarski, Manojkumar A. Puthenveedu

Department of Biological Sciences,

The Center for the Neural Basis of Cognition,

Carnegie Mellon University

Pittsburgh, PA 15213

Molecular Pharmacology Fast Forward. Published on February 2, 2017 as DOI: 10.1124/mol.116.106633
This article has not been copyedited and formatted. The final version may differ from this version.

MOL #106633

Running title: Endocytic lifetimes determine arrestin-mediated signaling by opioids

Corresponding Author:

Manojkumar Puthenveedu

Department of Biological Sciences

4400 Fifth Avenue MI202,

Carnegie Mellon University

Pittsburgh, PA 15213

Ph: 412 268 8236

Fax: 412 268 7129

Email: map3@andrew.cmu.edu

26 Pages (Abstract - Acknowledgements)

5 Figures + visual abstract

81 References

Abstract - 211 Words

Introduction - 728 Words

Discussion - 1479 Words

Abbreviations: β2AR - β2-adrenoreceptor; CB1R - cannabinoid receptor 1; CCP - clathrin-coated pit; CME - clathrin-mediated endocytosis; EKAR - ERK Kinase Activity Report;

ERK1/2 - extracellular regulate kinases 1 and 2; EM2 - endomorphin-2; FRET - Förster Resonance Energy Transfer; MS - morphine sulfate; GPCR - G-protein coupled receptor; siRNA - short-interfering RNA; SpH - superecliptic phluorin; SSF - signal sequence/FLAG; μR - μ receptor;

Abstract

Functional selectivity at the μ opioid receptor (μR), a prototypical GPCR that is a physiologically relevant target for endogenous opioid neurotransmitters and analgesics, has been a major focus for drug discovery in the recent past. Functional selectivity is a cumulative effect of the magnitudes of individual signaling pathways, e.g., the $G\alpha_i$-mediated and the arrestin-mediated pathways for μR. The present work tested the hypothesis that lifetimes of agonist-induced receptor-arrestin clusters at the cell surface controls the magnitude of arrestin signaling, and therefore functional selectivity, at μR. We show that endomorphin-2 (EM2), an arrestin-biased ligand for μR, lengthens surface lifetimes of receptor-arrestin clusters significantly compared to morphine. The lengthening of lifetimes required two specific leucines on the C-terminal tail of μR. Mutation of these leucines to alanines decreased the magnitude of arrestin-mediated signaling by EM2 without affecting G-protein signaling, suggesting that lengthened endocytic lifetimes were required for arrestin-biased signaling by EM2. Lengthening surface lifetimes by pharmacologically slowing endocytosis was sufficient to increase arrestin-mediated signaling by both EM2 and the clinically relevant agonist morphine. Our findings show that distinct ligands can leverage specific sequence elements on μR to regulate receptor endocytic lifetimes and the magnitude of arrestin-mediated signaling, and implicate these sequences as important determinants of functional selectivity in the opioid system.

Introduction

Although canonically called G-Protein Coupled Receptors (GPCRs), GPCRs can signal through diverse pathways after ligand binding (Pierce *et al.*, 2002; Belcheva *et al.*, 2005; DeWire *et al.*, 2007). GPCR activation by ligands induces conformational changes, allowing initial signaling through G proteins (Pierce et al., 2002) and phosphorylation by G protein-coupled receptor kinases, generating a phosphorylation barcode that is recognized by beta-arrestins (Premont and Gainetdinov, 2007; Nobles *et al.*, 2011). Arrestins are important effectors of GPCRs outside of G proteins, modulating both their trafficking and signaling (Shenoy and Lefkowitz, 2011; Goodman *et al.* 1996). Arrestins scaffold diverse downstream kinases, including Src and ERK1/2, on activated GPCRs to initiate G protein-independent signaling (Luttrell *et al.*, 1999; DeWire *et al.*, 2007; Shenoy and Lefkowitz, 2011).

Signaling bias between G-protein and arrestin-dependent pathways is an area of increasing interest in pharmacology (Urban *et al.*, 2007; Lefkowitz *et al.*, 2014; Zhou and Bohn, 2014). This functional selectivity, or biased agonism, has therapeutic potential, as specific pathways are being linked to specific physiological effects (Law *et al.*, 2013; Luttrell *et al.*, 2015; Chang and Bruchas, 2014; Kenakin, 2015). Functional selectivity is relevant especially in the field of opioid physiology. The μ receptor (μR), the primary target of most clinically relevant analgesics, can signal via both G-proteins and arrestins to cause complex physiological effects (Williams *et al.*, 2013; Thompson *et al*., 2015; Raehal *et al.*, 2011). Initial indications for functional selectivity came when morphine was shown to cause poor arrestin recruitment and internalization compared to endogenous opioids (Keith *et al.*, 1996; Sternini *et al*., 1996; Whistler and von Zastrow, 1998). This was substantiated by arrestin knockout in mice, which

Molecular Pharmacology Fast Forward. Published on February 2, 2017 as DOI: 10.1124/mol.116.106633
This article has not been copyedited and formatted. The final version may differ from this version.

attenuated a subset of physiological effects of opioids (Thompson *et al*., 2015; Raehal *et al.*, 2011). Recently, biased μR ligands that separate the beneficial and adverse effects of opioids have shown great therapeutic potential (Violin *et al*. 2014; Manglik *et al.*, 2016). Importantly, ligand bias is a function of the strengths of each signaling pathway, and the absolute magnitude of each pathway determines the downstream effects. This raises the possibility that the bias of a given drug can be controlled by changing the magnitude of individual pathways through which it signals.

The mechanisms by which ligands bias μR signaling are not clear. Research has focused on conformational changes and post-translational modifications that change the affinity of arrestin-μR interactions (Azzi *et al.*, 2003; Bradley and Tobin, 2016; Yu *et al* 1997; Rivero et al., 2012). It is evident, however, that the subcellular location of receptors is equally important, as it can significantly change the downstream effectors to which receptors couple (Ferrandon *et al.* 2009; Jean-Alphonse *et al.* 2014; Tsvetanova and von Zastrow, 2014; Bowman *et al.* 2016). Whether and how receptor trafficking influences functional selectivity of opioids is still unexplored.

In this context, μR and arrestin interact primarily in well-defined endocytic domains in cells. After arrestin recruitment, μR-arrestin complexes either recruit the endocytic protein clathrin, or are translocated to clathrin-coated pits (CCPs) (Wolfe and Trejo, 2007; Shenoy and Lefkowitz, 2011; Whistler and von Zastrow, 1998). This is followed by a highly ordered process of growth, maturation, and scission of the CCP, termed clathrin-mediated endocytosis (CME) (Taylor *et al.*, 2011; McMahon and Boucrot, 2011; Traub and Bonifacino, 2013; Cocucci *et al.*, 2014). GPCRs themselves can directly modulate CME dynamics (Puthenveedu and von Zastrow,

2006; Henry *et al.*, 2012; Soohoo and Puthenveedu, 2013; Lampe *et al.*, 2014; Flores-Otero *et al.*, 2014). μR actively regulates CCP scission via short amino acid motifs in its C-terminal intracellular tail (Soohoo and Puthenveedu, 2013), but the roles of these novel sequence elements in regulating μR function are not known.

Here we tested the hypothesis that these sequence elements determine the magnitude of arrestin signaling, and therefore functional selectivity of μR by regulating the dynamics of receptor endocytosis. Our results show that endomorphin-2 (EM2), an arrestin-biased ligand for μR, lengthens surface lifetimes significantly compared to morphine. This regulation required a specific sequence on the C-terminal tail of μR. Sequence-dependent lengthening of lifetimes was required for arrestin-biased signaling by EM2. Lengthening surface lifetimes by independently slowing endocytosis was sufficient to increase the magnitude of arrestin signaling, but not G protein signaling. Our findings implicate receptor surface lifetimes, controlled by a specific bi-leucine sequence on the μ receptor, as an important factor in regulating arrestin signaling without changing G protein signaling in the opioid system.

Molecular Pharmacology Fast Forward. Published on February 2, 2017 as DOI: 10.1124/mol.116.106633
This article has not been copyedited and formatted. The final version may differ from this version.

Material and Methods

Cell Culture and DNA Constructs

All experiments were performed with HEK 293 cells (American Tissue Culture Collection, Manassas, VA). Cells were cultured in DMEM (Fisher Scientific) with 10% FBS (Thermo Scientific). All plasmid transfections were conducted with Effectene (Qiagen) per manufacturer's instructions. Receptor constructs SSF-μR, SpH-μR, SpH-μR-LLAA, and SSF-μR-LLAA were all described previously (Soohoo and Puthenveedu, 2013). Stable cell lines expressing one of the above constructs were generated using Geneticin (Thermo Scientific) as selection reagent. cEKAR was a gift of Oliver Pertz (Addgene plasmid #39835, (Fritz *et al.*, 2013)), and nEKAR was generated from that plasmid by EcoRV restriction digest followed by religation to remove the nuclear export signal. β-arrestin2-GFP was previously described (Puthenveedu and von Zastrow, 2006). EPAC cAMP sensor has been previously described (DiPilato *et al.*, 2004). Endomorphin-2 and morphine (Sigma Aldrich, St. Louis, MO) were prepared as 10mM stocks in sterile water and used at 10μM. Dynasore (Sigma Aldrich) was prepared as 40mM stock in DMSO and used at 40μM. Knockdown of β-arrestin1 and 2 were conducted using 50pmol of 4 pooled siRNA sequences targeted to each isoform (Cat Nos. L-007292-00-0005 and L-011971-00-0005, GE Dharmacon), and cotransfected with EKAR sensors using Lipofectamine (Thermo Scientific). Control siRNA (sequence: GACCAGCCATCGTAGTACTTT) was synthesized using Ambion siRNA Silencer Construction Kit (Thermo Scientific). Arrestin knockdown was assessed using pan-Arrestin antibody (Cat No. PA1-730, Pierce Protein Biology, Rockford, IL, used at 1:1000), with lysates

run on a stain-free 4-20% gradient SDS-PAGE gel (Bio-Rad, Hercules, CA) and stain-free images taken to ensure equal load before transferring to nitrocellulose membrane.

EKAR FRET Assays

Cells stably expressing a construct of μR were transfected with either cEKAR or nEKAR (300ng). Cells were passed to coverslips, then imaged 2-3 days post transfection at roughly 50% confluency. Prior to imaging, cells were serum starved for 4 hours by removing growth medium, washing gently with DPBS twice, and then adding 1ml of L-15 medium. Cells were incubated with Alexa647-conjugated M1 antibody (Thermo Scientific; Sigma Aldrich) for 10 minutes to label SSF-μR. Cells were imaged at 37℃ using a Nikon Eclipse Ti automated inverted microscope, using a 60x/1.49 Apo-TIRF Objective (Nikon Instruments, Melville, NY). Cells were excited using 405 or 647nm solid-state lasers and every 30s images were collected for CFP (405nm excitation, 470/50 emission filter), FRET (405nm excitation, 530lp emission filter), and Alexa647 (647nm excitation, 700/75 emission) using an iXon+ 897 EMCCD camera (Andor, Belfast, UK). Cells were incubated with serum-free media for 5 minutes to establish baseline FRET response and then were stimulated with drug for 25 minutes. Images were exported as 16-bit tiff stacks and analyzed in ImageJ (NIH). Images were automatically thresholded and then the FRET channel was used to generate a cell mask. Images underwent a Gaussian blur (sigma=2px) to remove heterogeneity in signal introduced by delay between CFP and FRET channel correction, and then FRET channel was divided by CFP channel for each frame to

Molecular Pharmacology Fast Forward. Published on February 2, 2017 as DOI: 10.1124/mol.116.106633
This article has not been copyedited and formatted. The final version may differ from this version.

determine the FRET ratio. All resulting ratios were normalized to average ratio during baseline, with all values displayed here a measure of fractional increase in FRET ratio over baseline.

EPAC FRET Assays

Cells stably expressing μR were transfected with EPAC sensor (300ng) and imaged two days later. To allow for maximal cAMP production, cells were preincubated for 2 hours prior to imaging in L-15 media containing 1% FBS and 300μM IBMX to inhibit phosphodiesterase activity. Imaging was conducted as above. After 5 minute baseline, cells were exposed to 1μM forskolin to induce maximal cAMP production and then 5 minutes later, EM2 was added. Analysis was conducted as above, except that the calculated ratios given the in the paper are CFP/FRET.

Surface Lifetime Assays

Cells stably expressing μR were transfected with β-arrestin2-GFP (100ng) and imaged 2-3 days later. Imaging utilized the same setup as above, however this time also with a Nikon TIRF module. Cells were selected for imaging based on minimal initial visible arrestin fluorescence to increase SNR of arrestin puncta. Images for arrestin (488nm excitation, 525/50 emission) and the receptor (647nm excitation, 700/75 emission) were taken every 3s. Cells were allowed to equilibrate to imaging conditions for 1 minute before drug addition. Images were analyzed manually in ImageJ by tracking puncta between frames to determine their surface lifetime – a spot was only considered for manual analysis if it's appearance and disappearance

could be clearly visualized and it underwent minimal lateral movement. Images also underwent automated analysis, utilizing the cmeAnalysisPackage available from the Danuser lab (Aguet *et al.*, 2013) with minor updates to allow compatibility with newer versions of MATLAB (all code with modifications available at github.com/exark/cmeAnalysisPackage). The arrestin channel was used as the master and all lifetimes reported are based on category I, II and V tracks as detected by the software as these categories were required to include all previously manually identified tracks.

Phospho-ERK1/2 Blots

Cells stably expressing either WT- or LLAA-μR were plated at a density of 3.33 x 10^4/cm^2 and allowed to grow overnight in DMEM with 10% FBS. Cells were starved in serum-free DMEM for 4 hours prior to lysis. Cells were pretreated with either dynasore (40μM) or DMSO for 20 minutes before drug addition. After drug treatment, cells were incubated for stated period of time, then placed on ice and lysed and scraped in the plate with 2X RSB (Bio-Rad, Hercules, CA). Lysates were run on 4-20% stain-free gels, and stain-free images to total protein load were acquired before overnight transfer from gel to nitrocellulose membrane. Membranes were blocked in 5% BSA (Sigma Aldrich) and then probed for phospho-ERK1/2 (Cat No. 4370, Cell Signaling Technology, Danvers, MA, used at 1:1000). After blots were developed, they were subsequently stripped for 3 hours, then reblocked with 5% milk and probed for total ERK1/2 levels (Cat No. 4695, Cell Signaling Technology used at 1:1000). Densitometry was calculated in Image Lab (Bio-Rad), each lane's pERK signal was normalized to its total

Molecular Pharmacology Fast Forward. Published on February 2, 2017 as DOI: 10.1124/mol.116.106633
This article has not been copyedited and formatted. The final version may differ from this version.

ERK signal, and then normalized to no-treatment condition. Normalized replicates were averaged and are reported as group means ± SEM.

Statistical Analyses

All boxplots displayed in figures are displayed as box from 25th-quartile to 75th-quartile, with a line for the median, and the minimum and maximum displayed at the ends of the whiskers. Graphs with a single bar for each group are reported as mean ± standard error of the mean. For EKAR experiments, all calculations were conducted using Prism 6 (GraphPad). Individual cells were included in these analyses if they showed at least three consecutive data points during the treatment with a consistent increase over the average baseline measurement. Peak response values are taken as the max value during treatment phase of trial. Area under the curve is calculated for treatment phase of trial, using 1.0 as a baseline measure. AUCs from individual cells were averaged to establish group means. Statistical comparisons for data presented in boxplots was conducted using Mann-Whitney U tests, comparisons for data displayed in bar graphs was done using a t-test with Welch's correction. Comparisons of peak and AUC data were evaluated against a Šidák-corrected p-value of 0.0253 to keep familywise error at less than 5% for these multiple comparisons. Comparisons where ANOVA was used are specifically noted, with post-hoc comparisons between the means of indicated groups having been conducted to test for significance.

For clustering experiments, manual surface lifetime measurements were averaged to produce population means and means were compared with two sample t-test with Welch's

Molecular Pharmacology Fast Forward. Published on February 2, 2017 as DOI: 10.1124/mol.116.106633
This article has not been copyedited and formatted. The final version may differ from this version.

correction in Prism. Fraction of clusters with lifetimes greater than 150s were averaged across cells and are reported as group means ± SEM. Cumulative distributions of clusters with lifetimes greater than 150s from automated analysis were compared using a two sample Kolmogorov-Smirnov test for distribution independence using the function kstest2 in MATLAB (MathWorks), with the corresponding p-value and KS statistic reported.

Molecular Pharmacology Fast Forward. Published on February 2, 2017 as DOI: 10.1124/mol.116.106633
This article has not been copyedited and formatted. The final version may differ from this version.

Results

Endomorphin-2 induces longer surface lifetimes of receptor-arrestin clusters and greater arrestin-mediated ERK1/2 activation compared to morphine

We hypothesized that if the time the receptor spends at the cell surface after agonist treatment (surface lifetime) colocalized with arrestin affects arrestin-mediated signaling magnitude, we should see disparate lifetimes in ligands depending on the magnitude of arrestin recruitment a ligand was capable of producing. Endomorphin-2 (EM2) was selected as an example of an endogenous ligand for μR that is able to strongly recruit arrestin (Rivero *et al.*, 2012) , and morphine (MS) was selected as a model ligand with a demonstrated ability to poorly recruit arrestin to the receptor (Zheng *et al.*, 2008; Raehal *et al.*, 2011, McPherson *et al.*, 2010).

To investigate the magnitude of arrestin-dependent signaling produced by these two ligands we assayed for ERK1/2 activation, a well-documented downstream effector of arrestin (Luttrell and Lefkowitz, 2002, DeWire *et al.*, 2007). HEK 293 cells stably expressing a construct of the murine μR with an N-terminal FLAG epitope were treated with saturating concentrations (10μM) of either EM2 or morphine for 5 minutes and then lysed. Subsequent immunoblotting revealed a subtle but significant increase in ERK1/2 phosphorylation for EM2 treatment compared to morphine (Supplemental Figure 1). To achieve better temporal and spatial sensitivity, we used the Förster resonance energy transfer (FRET) biosensor EKAR (Fritz *et al.*, 2013) to assay for ERK1/2 activation in live cells. The same cell line used for immunoblotting was transiently transfected with either the cytosolic- or nuclear-localized variants of EKAR (cEKAR and nEKAR, respectively). Cells were labeled with an Alex647-conjugated M1-FLAG

antibody and then imaged live to visualize receptor internalization and FRET ratio changes following agonist treatment (Figure 1A & B, 1G & H).

Both in the nucleus and in the cytosol, ERK activity peaked about 5 minutes after agonist addition for both agonists (see Figure 1C & 1I for example traces). EM2 produced a greater peak ERK1/2 response in both the nucleus and the cytosol (Figure 1D, 1J). The same trend of greater EM2-elicited activation compared to morphine was seen when measuring total ERK1/2 response by taking the area under the curve of each response, with EM2 producing a greater total response than morphine in both cytosol and nucleus (Figure 1E, 1K). In the cytosol, the difference in total ERK response was further pronounced than in the nucleus due to a second phase of ERK activation that was only present for EM2 and not for morphine (Figure 1I). This is consistent with prior data suggest that arrestin signaling induces a temporally distinct wave of ERK signaling.

To assess the contribution of arrestin-dependent signaling on the difference in ERK1/2 activation between morphine and EM2, we performed a double knockdown of β-arrestin1 and β-arrestin2 and then measured ERK response with EKAR. Knockdown was confirmed via immunoblot, with the arrestin signal normalized to total protein from a stain-free gel image (Fig 1Fi, see Methods for further details). For EM2, arrestin knockdown significantly decreased peak signaling in the cytosol and in the nucleus (Figure 1F, 1L), with a specific effect of reducing the second peak. Arrestin knockdown did not have a significant effect on morphine-dependent ERK activation. This suggests that the difference in ERK1/2 activation between these two agonists is primarily controlled by arrestin-dependent signaling.

Molecular Pharmacology Fast Forward. Published on February 2, 2017 as DOI: 10.1124/mol.116.106633
This article has not been copyedited and formatted. The final version may differ from this version.

Given the arrestin dependence of the difference in ERK signaling between morphine and EM2, we investigated whether these agonists induced differential lifetimes of receptor clusters with arrestin. Previous work has demonstrated that clusters of μR that form in response to DAMGO, another endogenous agonist of the receptor, persist at the cell membrane for a protracted duration, with an average lifetime of 100s (Henry *et al.*, 2012; Soohoo and Puthenveedu, 2013). We investigated the extent to which morphine vs. EM2 controlled the lifetime of receptor clusters, and specifically whether arrestin colocalized with receptor for the duration of its lifetime.

We imaged HEK 293 cells stably expressing FLAG-μR, transfected with low levels of an EGFP-tagged β-arrestin2 construct, using TIR-FM, to visualize arrestin-μR colocalization after agonist addition. For EM2, long-lived receptor clusters were easily visible and arrestin colocalized with receptor clusters for their entire surface lifetime (Figure 2A). Similar colocalization was seen with morphine (Figure 2B). Receptor clustering was also evident in response to morphine, consistent with previous reports in cells expressing arrestin (Whistler and von Zastrow, 1998), with arrestin clusters colocalizing with μR (Figure 2C). Automated analysis of clustering movies allowed quantification of receptor and arrestin fluorescence over time, with results showing that regardless of cluster lifetime, arrestin and receptor presence at clusters coincided for the lifetime of the cluster (Figure 2D). Surface lifetimes of arrestin clusters were measured manually as explained in Methods and as described previously (Puthenveedu and von Zastrow, 2006; Soohoo and Puthenveedu, 2013). The lifetimes of EM2-dependent arrestin clusters were longer compared to morphine. EM2 produced a maximum arrestin cluster lifetime of 378 s and a median of 87s compared to a maximum of 72 s and median of 32 s for morphine

(Figure 2E). Average lifetimes for arrestin clusters across the population were significantly longer for EM2 compared to morphine (97.93±4.501 for EM2 vs. 35.40±1.393), correlating with the difference seen in ERK1/2 activation between the two ligands (Figure 2F).

We next used an objective and automated image analysis method to measure surface lifetimes, to provide an unbiased analysis of all endocytic clusters across the whole experimental data set. To do this, we adapted an available automated toolset for measuring lifetimes of diffraction limited spots from TIR-FM movies (Aguet *et al.*, 2013) to measure the difference in lifetime between the two agonists. As reported previously, the absolute values of population dynamics differed from the manual analysis, with the automated analysis identifying a much larger fraction of shorter lived clusters than are identified through manual methods (Loerke *et al.*, 2009; Liu *et al.*, 2010; Aguet *et al.*, 2013; Soohoo and Puthenveedu, 2013; Mettlen and Danuser, 2014; Hong *et al.*, 2015; Doyon *et al.*, 2011). Nevertheless, the automated analysis recapitulated the longer lifetimes seen for EM2 compared to morphine, particularly evident in a greater frequency of longer lived pits of above 150s in duration (Figure 2G). This difference is apparent as an overall rightward shift of the EM2 lifetime cumulative distribution compared to morphine (Figure 2H).

Lengthened surface lifetimes are required for maximal ERK1/2 signaling by endomorphin-2

Our above results indicate that the duration that arrestin colocalizes with μR during internalization correlates with the magnitude of arrestin signaling. To test whether there is a

causal relationship between surface lifetime and arrestin signaling, we first asked whether increased EM2 signaling via arrestin required long-lived receptor clusters.

To investigate this, we used a specific mutant of μR (LLAA μR, L389A, L392A), that internalizes quickly and has previously been shown to have a short lifetime in response to DAMGO compared to WT μR (Soohoo and Puthenveedu, 2013). We used TIR-FM to visualize clustering and arrestin-colocalization dynamics of cells stably expressing either WT or LLAA μR treated with EM2. Importantly, EM2-treated LLAA μR behaved similar to morphine-treated WT μR in activation and arrestin recruitment. However, the heterogeneity of the overall lifetimes of arrestin clusters was greatly diminished in the mutant compared to the WT receptor (Figure 3A). LLAA μR also had a significantly shorter mean lifetime of arrestin clusters after agonist addition (Figure 3B). Additionally, the automated analysis showed a distinction between WT and LLAA μR with the WT receptor accruing a greater fraction of arrestin clusters with lengthy lifetimes (Figure 3C) as well as having a significant rightward shift of its cumulative distribution curve (Figure 3D). Combined with our earlier data with DAMGO, these data with EM2 indicate that L389 and L392 of μR are required for increasing surface lifetime of receptor-arrestin clusters after activation.

Importantly, there were no differences in overall arrestin recruitment between the WT and LLAA μR. When cells expressing WT or LLAA μR and a tdTomato-tagged β-arrestin2 construct were imaged using TIR-FM with high time resolution (10Hz), arrestin recruitment appeared comparable across cells (Figure 3E), with clusters appearing at roughly commensurate times in each cell line. To quantify the kinetics of arrestin recruitment, these movies were analyzed using automated analysis to identify clusters. When fluorescence intensities for

Molecular Pharmacology Fast Forward. Published on February 2, 2017 as DOI: 10.1124/mol.116.106633
This article has not been copyedited and formatted. The final version may differ from this version.

individual clusters were measured across many clusters, the time to plateau of cluster fluorescence was uniformly about 6s, and slopes were identical between WT and LLAA μR-expressing cells (Figure 3F). These results show that the LLAA μR mutant recruited arrestin to comparable levels, but showed shorter surface lifetimes. This provided an excellent model to test whether increased EM2 signaling via arrestin requires long-lived receptor clusters.

To test whether shortened lifetimes changed the magnitude of arrestin-mediated signaling, we measured ERK1/2 activation caused by LLAA μR upon EM2 treatment. Peak ERK1/2 activation was significantly higher for WT μR compared to LLAA μR in the cytosol (cEKAR, Figure 4A), with the same trend in total response (Figure 4B). This difference is repeated and accentuated in the nucleus, with WT μR showing a larger increase compared to LLAA μR for both peak and total ERK response (nEKAR, Figure 4C, 4D). The ERK responses of LLAA μR with EM2 were roughly comparable to that of the WT μR with morphine (Figure 4C vs 1C, 4D vs 1H). These results indicate that μR-mediated extension of surface lifetime is required for maximal arrestin-mediated ERK1/2 signaling.

We next tested whether this relationship between surface lifetimes and ERK signaling was conserved across different agonists with different magnitudes of arrestin and G protein signaling. We selected agonists able to recruit arrestin strongly (EM2, DAMGO), moderately (fentanyl, methadone), and weakly (morphine, oxycodone) (McPherson *et al.* 2010), and tested the responses of WT and LLAA μR in the EKAR assay. To measure signaling differences, we calculated mean total ERK response (AUC) to each agonist for both WT and LLAA μR. We then subtracted the LLAA mean from the WT mean to determine the difference score, or magnitude of ERK activation difference across the two receptors, as an index of the contribution of surface

Molecular Pharmacology Fast Forward. Published on February 2, 2017 as DOI: 10.1124/mol.116.106633
This article has not been copyedited and formatted. The final version may differ from this version.

lifetimes to ERK response. Strikingly, the magnitude of difference between WT and LLAA μR paralleled the abilities of the ligands to recruit arrestin (Figure 4E), indicating that the contribution of extended lifetimes was restricted to arrestin-mediated signaling.

To directly determine whether changes in lifetimes regulated G-protein dependent signaling, we compared G-protein responses between WT and LLAA μR after EM2. As μR is $G\alpha_{i/o}$-coupled, we assayed receptor-dependent inhibition of cAMP production using the FRET biosensor EPAC (DiPilato *et al.*, 2004). Cells stably expressing either WT or LLAA μR were transiently transfected with EPAC. Cells were subsequently imaged live (Figure 4F & G). Forskolin (FSK) was used to stimulate cAMP production, and then after 5 minutes EM2 was added to induce inhibition of cAMP production. EM2 induced a rapid decrease in FRET ratio in the case of both receptors (Figure 4H for example traces), and the overall magnitude of the inhibition was comparable between the two receptor variants (Figure 4I). These results indicate that WT and LLAA μR have comparable EM2-dependent G-protein activation, showing that, consistent with our model, the differences in surface lifetimes of receptor arrestin clusters specifically drive differences in the ERK1/2 pathway.

Lengthening surface lifetimes of receptor arrestin clusters is sufficient to increase μR-mediated ERK1/2 signaling

We next determined whether extending lifetimes of LLAA μR was sufficient to increase its ERK1/2 signaling**.** To test the sufficiency of lengthened lifetimes to increase ERK1/2 signaling, we delayed the endocytosis of LLAA μR by pretreating cells with 40μM dynasore.

Dynasore is a known inhibitor of endocytosis, with previous work showing that ~80μM final concentration of the drug is enough to block almost 90% of clathrin-mediated endocytic cargo (Macia *et al.*, 2006). As we sought to merely mimic the effects of WT μR and lengthen lifetimes instead of blocking internalization entirely, we utilized 40μM dynasore pretreatment to slow endocytic scission. Example kymographs show the increase in lifetimes for LLAA μR (Figure 5A). We measured an increase in population lifetimes, showing that dynasore treatment had the desired effect in increasing both median lifetime and heterogeneity of population lifetimes for LLAA μR (Figure 5B).

We next used LLAA to test whether increasing lifetimes was sufficient to increase the magnitude of ERK signaling. We initially attempted to use the EKAR assay to demonstrate changes in ERK activation. Dynamin inhibitors such a dynasore, in our hands, produces considerable autofluorescence in the FRET fluorescence channel (Supplemental Figure 2) that reduced the signal-to-noise enough that we could not detect any differences. We therefore investigated the effects of dynasore on LLAA ERK signaling using an immunoblots to detect phospho-ERK (pERK).. Cells stably expressing LLAA μR were either pretreated with 40μM dynasore, or DMSO as a control, for 20 minutes, and then exposed to EM2 for 5 minutes. Cells were subsequently lysed and assayed for pERK1/2 levels. Dynasore pretreatment had no effect on basal ERK1/2 phosphorylation, but significantly increased EM2-dependent ERK1/2 activation compared to untreated cells (Figure 5C). These results indicate that lengthened cluster lifetimes are sufficient to increase ERK1/2 signaling.

Given the results seen with EM2 at the short-lifetime μR mutant, we next tested whether lengthening lifetimes was sufficient to allow morphine to activate ERK1/2 efficiently. In cells

Molecular Pharmacology Fast Forward. Published on February 2, 2017 as DOI: 10.1124/mol.116.106633
This article has not been copyedited and formatted. The final version may differ from this version.

pretreated with dynasore, morphine caused higher ERK1/2 activation, as evidenced by higher pERK levels, after 5 minutes. This result shows that lengthened lifetime is sufficient to increase ERK1/2 activation. Together, our data indicate that the lifetime of receptor-arrestin clusters on the cell surface determines the strength of arrestin signaling, and therefore the functional selectivity of ligands between G-protein and arrestin pathways.

Molecular Pharmacology Fast Forward. Published on February 2, 2017 as DOI: 10.1124/mol.116.106633
This article has not been copyedited and formatted. The final version may differ from this version.

Discussion

Our results show that the μ receptor uses specific sequences on its C-terminus to regulate the magnitude of its arrestin-mediated signaling by delaying endocytosis and lengthening the lifetimes of receptor-arrestin clusters on the cell surface. Lengthened surface lifetimes were required (Fig 4 A-D) and sufficient (Fig 5 A-C) for maximal arrestin signaling from the receptor. The strength of G protein signaling, in contrast, was not affected by lifetimes (Fig 4 F-I). This suggests that sequence-dependent regulation of surface lifetimes regulates arrestin signaling at μR without changing G protein signaling to control functional selectivity.

Surface lifetimes could be a mechanism to tune the functional selectivity of ligands independent of their intrinsic bias. Ligand-dependent differences in the magnitude of arrestin signaling and in functional selectivity at μR are well documented, although the mechanisms are still not well understood (Williams *et al.* 2013, Raehal *et al.* 2014). For example, using elegant FRET-based assays, μR was recently shown to cluster in distinct membrane domains on the cell surface in response to the ERK EC_{50} doses of morphine (100nM) and DAMGO (10nM), leading to differential nuclear and cytoplasmic ERK signaling (Halls *et al.* 2016). Clustering was not directly tested in these experiments, and our experiments, performed with saturating doses at imaging resolutions that directly detects clustering, resolve the functional nature of these domains. Although 100nM morphine did not cause nuclear ERK activation (Halls *et al.* 2016), our experiments with saturating morphine showed nuclear signals, consistent with previous work (Zheng *et al.* 2008). Interestingly, while ERK activation has been linked primarily to cell proliferation and migration (Strungs and Luttrell 2014), ERK activation in the midbrain or striatum neurons, which are not proliferative, modifies the addictive properties of opioids

(Macey *et al.* 2009, Lin *et al.* 2010). The differences between experiments may therefore aso represent a physiological divergence of ERK signaling downstream of different agonists.

Different agonists could leverage this ability of surface lifetimes to influence arrestin-mediated signaling. Morphine, a ligand that induces shorter surface lifetimes of μR and arrestin clusters, produces a lower magnitude of arrestin signaling compared to EM2, which induces longer lifetimes (Fig 1 and 2). Lengthening lifetimes was sufficient to increase the magnitude of arrestin signaling produced by morphine (Figure 5E & F). Interestingly, different μR agonists differ in the ability to recruit arrestin (Whistler and von Zastrow, 1998, Williams et al., 2013, McPherson *et al.* 2010), and this correlated well with the dependence on lifetimes for arrestin signaling, implicating surface lifetime as a modulator of arrestin-dependent signaling (Figure 4E). It remains unclear whether arrestin itself mediates these extended lifetimes. Our work using the LLAA μR mutant, whose ability to recruit arrestin does not differ from the WT receptor for the same agonist (Figure 4E & F), suggests that endocytic delay can be separated from arrestin recruitment. Nevertheless, the differences might be driven by differential μR phosphorylation patterns controlled by different ligands (Doll *et al.* 2011, Doll *et al.* 2012, Tobin *et al.* 2008). It is possible that LLAA, because the C-terminal tail affects receptor phosphorylation patterns (Zindel *et al.* 2015), shows a different phosphorylation pattern than the WT μR, similar to what is caused by different ligands.

Irrespective of the mechanism, control of surface lifetimes by specific sequences on GPCRs might serve as a general timer for arrestin-mediated signaling from the surface. Such cargo-mediated control of surface lifetimes was first described for the β-adrenoceptors (Puthenveedu and von Zastrow, 2006), and has since been reported for μR and cannabinoid 1

receptor (CB1R) (Henry *et al.*, 2012; Soohoo and Puthenveedu, 2013; Lampe *et al.*, 2014; Flores-Otero *et al.*, 2014). In the case of CB1R, two different ligands - WIN 55,212-2 and 2-AG - caused differences in surface lifetimes as well as in arrestin signaling, consistent with our results (Flores-Otero *et al.*, 2014; Delgado-Peraza *et al.* 2016). The specific mechanisms used, however, might vary between different GPCRs. The β-adrenoreceptors use Type I PDZ-ligand sequences on their C-termini to lengthen lifetimes by delaying the recruitment of dynamin, a key mediator of endocytic scission (Puthenveedu and von Zastrow, 2006). μR, in contrast, uses a bi-leucine sequence to delay the time to scission after dynamin has been recruited (Soohoo and Puthenveedu, 2013). For the CB1R, recent work suggests that the primary determinant of surface lifetimes is the affinity of arrestin binding itself, dictated by phosphorylation of the receptor (Delgado-Peraza *et al.*, 2016). Although the specific factors used by different receptors to regulate surface lifetimes might differ, the general mechanism likely involves multi-protein interactions that stabilize components of the endocytic machinery.

PDZ domain-containing proteins are attractive candidates to provide a multi-domain scaffold for such interactions (Romero *et al.*, 2011; Dunn and Ferguson, 2015). Because PDZ-domain containing proteins can interact with the actin cytoskeleton, and because actin can regulate endocytic dynamics (Grassart *et al.*, 2014; Dunn and Ferguson, 2015), a straightforward possibility is that adrenoceptors regulate endocytosis by recruiting actin or modifying actin dynamics. Consistent with this idea, an actin-binding domain fused to the tail of GPCRs is sufficient to extend surface lifetimes of receptor clusters (Puthenveedu and von Zastrow, 2006). On μR, the bi-leucine sequence that regulates surface lifetimes and arrestin signaling (Fig 4 A-D) does not conform to an obvious PDZ ligand sequence, and has no known interactors. This

sequence might represent an internal PDZ ligand (Paasche *et al.*, 2005; Lee and Zheng, 2010), although this is unlikely, considering that μR delays lifetimes at a step distinct from adrenoceptors. CB1R might also be indirectly linked to PDZ proteins through its binding partner CRIP1 (Daigle *et al.*, 2008; Smith *et al.*, 2015). PDZ interactions are sufficient for regulating surface lifetimes (Puthenveedu and von Zastrow, 2006), but the relative contribution of PDZ interactions and arrestin affinities (Delgado-Peraza *et al.* 2016) in regulating CB1R endocytosis is not known. A general role for PDZ proteins in regulating functional selectivity is also consistent with reports that PDZ interactions can regulate endocytosis, arrestin recruitment, and ERK signaling by other GPCRs, although whether the effects are through regulating lifetimes is unclear (Yang *et al.*, 2010; Dunn and Ferguson, 2015; Walther *et al.*, 2015; Dunn *et al.*, 2016). One key consequence shared between all these GPCRs, however, is a prolonged interaction between arrestin and receptors on the surface. Arrestins are well-recognized regulators of GPCR signaling (Luttrell and Lefkowitz, 2002; Shenoy and Lefkowitz, 2011; Raehal and Bohn, 2014) and trafficking (Goodman *et al.*, 1996), and arrestin-GPCR interactions might be regulated in multiple ways.

These diverse roles of arrestins could result from their ability to adopt a variety of potential conformations and recruit different binding partners, depending on the conformation (Xiao *et al.*, 2007; Gurevich and Gurevich, 2014). Recent work shows that a single receptor can recruit arrestin in a variety of conformations depending on the ligand, leading to distinct signaling profiles (Lee *et al.*, 2016). It is unclear what dictates these conformations, but experiments with chimeric receptors show that the C-terminal tail of a receptor is sufficient. This suggests that amino acid motifs in the receptor (such as MOR's LENLEAE sequence) and/or

Molecular Pharmacology Fast Forward. Published on February 2, 2017 as DOI: 10.1124/mol.116.106633
This article has not been copyedited and formatted. The final version may differ from this version.

variable phosphorylation state can modulate arrestin conformation. Since arrestin interacts with endocytic components, conformational variability could determine the composition of the signaling complexes present in endocytic domains. This model agrees also with recent work highlighting new paradigms, where arrestin activation and clustering occurs independent of receptor interactions (Eichel *et al.* 2016), or highly transient receptor-arrestin interactions leave arrestin with a 'memory' of activation, leading to arrestin signaling complexes without receptor (Nuber *et al.*, 2016). Because μR colocalizes well with arrestin throughout the endocytic cycle (Fig 2A & B), however, the effects on arrestin signaling is likely evinced through prolonged association with the receptor.

Although the receptors identified to modulate surface lifetimes so far have been Class A receptors, which dissociate from arrestin concomitantly with endocytosis, modulating lifetime might have physiological consequences even for Class B GPCRs, which interact with arrestin for prolonged periods including on the endosome (Shenoy and Lefkowitz, 2011). Emerging data suggest that the location of signal origin is an important determinant of downstream consequences of GPCR activation. For the β2-adrenoceptor, $G\alpha_s$ signaling from microdomains on the endosome causes the activation of a subset of genes that are distinct from the genes activated by $G\alpha_s$ signaling on the surface (Irannejad *et al.*, 2013; Tsvetanova and von Zastrow, 2014). In the event that a similar paradigm exists for arrestin signaling, surface lifetimes would determine the surface to endosome spatial bias for Class B receptors. In this context, our result - that manipulation of receptor surface lifetimes can modulate the magnitude of arrestin signaling - provides a clear example of the potential to control GPCR physiology by manipulating the spatial location of receptors. This is an emerging concept in GPCR biology that builds on the

Molecular Pharmacology Fast Forward. Published on February 2, 2017 as DOI: 10.1124/mol.116.106633
This article has not been copyedited and formatted. The final version may differ from this version.

exciting idea that manipulation of receptor location could be a target for developing therapeutic strategies in the future to modulate and fine-tune the diverse effects of existing drugs.

Molecular Pharmacology Fast Forward. Published on February 2, 2017 as DOI: 10.1124/mol.116.106633
This article has not been copyedited and formatted. The final version may differ from this version.

Acknowledgements

The authors thank Drs. Peter A. Friedman, Guillermo G. Romero, Cheng Zhang, Adam D. Linstedt, and Sandra J. Kuhlman for valuable feedback over the course of the project. Members of the M.A.P. laboratory, particularly Dr. Shanna B. Bowman, provided essential feedback on the manuscript. Z.Y.W. would also like to thank Anthony F. Iommi for valuable help.

Molecular Pharmacology Fast Forward. Published on February 2, 2017 as DOI: 10.1124/mol.116.106633
This article has not been copyedited and formatted. The final version may differ from this version.

Author Contributions

Participated in research design: Weinberg, Zajac, and Puthenveedu.

Conducted experiments: Weinberg, Zajac, and Puthenveedu.

Contributed new reagents or analytic tools: Phan, and Shiwarski.

Performed data analysis: Weinberg, Zajac, Phan, and Puthenveedu.

Wrote or contributed to the writing of the manuscript: Weinberg, Zajac, and Puthenveedu.

References

Aguet F, Antonescu CN, Mettlen M, Schmid SL, and Danuser G (2013) Advances in analysis of low signal-to-noise images link dynamin and AP2 to the functions of an endocytic checkpoint. *Developmental Cell* **26**:279–291.

Allen JA, Yost JM, Setola V, Chen X, Sassano MF, Chen M, Peterson S, Yadav PN, Huang X-P, Feng B, Jensen NH, Che X, Bai X, Frye SV, Wetsel WC, Caron MG, Javitch JA, Roth BL, and Jin J (2011) Discovery of β-arrestin-biased dopamine D2 ligands for probing signal transduction pathways essential for antipsychotic efficacy. *Proc Natl Acad Sci USA* **108**:18488–18493,

Azzi M, Charest PG, Angers S, Rousseau G, Kohout T, Bouvier M, and Piñeyro G (2003) Beta-arrestin-mediated activation of MAPK by inverse agonists reveals distinct active conformations for G protein-coupled receptors. *Proceedings of the National Academy of Sciences* **100**:11406–11411.

Belcheva MM, Clark AL, Haas PD, Serna JS, Hahn JW, Kiss A, and Coscia CJ (2005) Mu and kappa opioid receptors activate ERK/MAPK via different protein kinase C isoforms and secondary messengers in astrocytes. *Journal of Biological Chemistry* **280**:27662–27669.

Benovic JL, Kühn H, Weyand I, Codina J, Caron MG, and Lefkowitz RJ (1987) Functional desensitization of the isolated beta-adrenergic receptor by the beta-adrenergic receptor kinase: potential role of an analog of the retinal protein arrestin (48-kDa protein). *Proceedings of the National Academy of Sciences* **84**:8879–8882.

Bowman SL, Shiwarski DJ, and Puthenveedu MA (2016) Distinct G protein-coupled receptor

recycling pathways allow spatial control of downstream G protein signaling. *The Journal of Cell Biology* **214**:797–806.

Bradley SJ, and Tobin AB (2016) Design of Next-Generation G Protein–Coupled Receptor Drugs: Linking Novel Pharmacology and In Vivo Animal Models. *Annu Rev Pharmacol Toxicol* **56**:535–559.

Chang SD, Bruchas MR (2014) Functional selectivity at GPCRs: new opportunities in psychiatric drug discovery. *Neuropsychopharmacology* **39**:248-249.

Cocucci E, Gaudin R, and Kirchhausen T (2014) Dynamin recruitment and membrane scission at the neck of a clathrin-coated pit. *Molecular Biology of the Cell* **25**:3595–3609

Daigle TL, Kwok ML, and Mackie K (2008) Regulation of CB1 cannabinoid receptor internalization by a promiscuous phosphorylation-dependent mechanism. *Journal of Neurochemistry* **106**:70–82.

Delgado-Peraza F, Ahn KH, Nogueras-Ortiz C, Mungrue IN, Mackie K, Kendall DA, and Yudowski GA (2016) Mechanisms of Biased β-Arrestin-Mediated Signaling Downstream from the Cannabinoid 1 Receptor. *Molecular Pharmacology* **89**:618–629.

DeWire SM, Ahn S, Lefkowitz RJ, and Shenoy SK (2007) Beta-arrestins and cell signaling. *Annu Rev Physiol* **69**:483–510.

DeWire SM, Yamashita DS, Rominger DH, Liu G, Cowan CL, Graczyk TM, Chen X-T, Pitis PM, Gotchev D, Yuan C, Koblish M, Lark MW, and Violin JD (2013) A G protein-biased ligand

at the μ-opioid receptor is potently analgesic with reduced gastrointestinal and respiratory dysfunction compared with morphine. *Journal of Pharmacology and Experimental Therapeutics* **344**:708–717.

DiPilato LM, Cheng X, and Zhang J (2004) Fluorescent indicators of cAMP and Epac activation reveal differential dynamics of cAMP signaling within discrete subcellular compartments. *Proceedings of the National Academy of Sciences* **101**:16513–16518.

Doyon JB, Zeitler B, Cheng J, Cheng AT, Cherone JM, Santiago Y, Lee AH, Vo TD, Doyon Y, Miller JC, Paschon DE, Zhang L, Rebar EJ, Gregory PD, Urnov FD, and Drubin DG (2011) Rapid and efficient clathrin-mediated endocytosis revealed in genome-edited mammalian cells. *Nat Cell Biol* **13**:331–337.

Doll C, Konietzko J, Pöll F, Koch T, Höllt V, and Schulz S (2011) Agonist-selective patterns of μ-opioid receptor phosphorylation revealed by phosphosite-specific antibodies. *Br J Pharmacol* **164**:298–307.

Doll C, Pöll F, Peuker K, Loktev A, Glück L, and Schulz S (2012) Deciphering μ-opioid receptor phosphorylation and dephosphorylation in HEK293 cells. *Br J Pharmacol* **167**:1259–1270.

Dunn HA, and Ferguson SSG (2015) PDZ Protein Regulation of G Protein-Coupled Receptor Trafficking and Signaling Pathways. *Molecular Pharmacology* **88**:624–639.

Dunn HA, Chahal HS, Caetano FA, Holmes KD, Yuan GY, Parikh R, Heit B, and Ferguson SSG (2016) PSD-95 regulates CRFR1 localization, trafficking and β-arrestin2 recruitment. *Cell Signal*

28:531–540.

Eichel K, Jullie D, and Zastrow von M (2016) β-Arrestin drives MAP kinase signalling from clathrin-coated structures after GPCR dissociation. *Nat Cell Biol* **18**:303–310.

Ferrandon S, Feinstein TN, Castro M, Wang B, Bouley R, Potts JT, Gardella TJ, and Vilardaga J-P (2009) Sustained cyclic AMP production by parathyroid hormone receptor endocytosis. *Nat Chem Biol* **5**:734–742.

Flores-Otero J, Ahn KH, Delgado-Peraza F, Mackie K, Kendall DA, and Yudowski GA (2014) Ligand-specific endocytic dwell times control functional selectivity of the cannabinoid receptor 1. *Nat Comms* **5**:4589.

Fritz RD, Letzelter M, Reimann A, Martin K, Fusco L, Ritsma L, Ponsioen B, Fluri E, Schulte-Merker S, van Rheenen J, and Pertz O (2013) A versatile toolkit to produce sensitive FRET biosensors to visualize signaling in time and space. *Sci Signal* **6**:rs12.

Grassart A, Cheng AT, Hong SH, Zhang F, Zenzer N, Feng Y, Briner DM, Davis GD, Malkov D, and Drubin DG (2014) Actin and dynamin2 dynamics and interplay during clathrin-mediated endocytosis. *The Journal of Cell Biology* 205:721–735.

Goodman OB, Krupnick JG, Santini F, Gurevich VV, Penn RB, Gagnon AW, Keen JH, and Benovic JL (1996) Beta-arrestin acts as a clathrin adaptor in endocytosis of the beta2-adrenergic receptor. *Nature* **383**:447–450.

Gurevich VV, and Gurevich EV (2014) Extensive shape shifting underlies functional versatility

of arrestins. *Current Opinion in Cell Biology* **27**:1–9.

Halls ML, Yeatman HR, Nowell CJ, Thompson GL, Gondin AB, Civciristov S, Bunnett NW, Lambert NA, Poole DP, Canals M (2016). Plasma membrane localization of the μ-opioid receptor controls spatiotemporal signaling. *Sci Signal.* **9**:ra16.

Hanyaloglu AC, and Zastrow MV (2008) Regulation of GPCRs by Endocytic Membrane Trafficking and Its Potential Implications. *Annu Rev Pharmacol Toxicol* **48**:537–568.

Henry AG, Hislop JN, Grove J, Thorn K, Marsh M, and Zastrow von M (2012) Regulation of Endocytic Clathrin Dynamics by Cargo Ubiquitination. *Developmental Cell* **23**:519–532.

Hong SH, Cortesio CL, and Drubin DG (2015) Machine-Learning-Based Analysis in Genome-Edited Cells Reveals the Efficiency of Clathrin-Mediated Endocytosis. *Cell Reports* **12**:2121–2130.

Irannejad R, Tomshine JC, Tomshine JR, Chevalier M, Mahoney JP, Steyaert J, Rasmussen SGF, Sunahara RK, El-Samad H, Huang B, and Zastrow von M (2013) Conformational biosensors reveal GPCR signalling from endosomes. *Nature* **495**:534–538.

Jean-Alphonse F, Bowersox S, Chen S, Beard G, Puthenveedu MA, and Hanyaloglu AC (2014) Spatially restricted G protein-coupled receptor activity via divergent endocytic compartments. *J Biol Chem* **289**:3960–3977.

Keith DE, Murray SR, Zaki PA, Chu PC, Lissin DV, Kang L, Evans CJ, von Zastrow M (1996) Morphine activates opioid receptors without causing their rapid internalization. *J Biol Chem*

271:19021-19024.

Kenakin T (2015) The Effective Application of Biased Signaling to New Drug Discovery. *Mol Pharmacol.* **88**:1055-1061.

Koch T and Höllt V (2008) Role of receptor internalization in opioid tolerance and dependence. *Pharmacol Ther* **117**:199–206.

Kroeze WK, Sassano MF, Huang X-P, Lansu K, McCorvy JD, Giguere PM, Sciaky N, and Roth BL (2015) PRESTO-Tango as an open-source resource for interrogation of the druggable human GPCRome. *Nature Publishing Group* **22**:362–369.

Krupnick JG, and Benovic JL (1998) The role of receptor kinases and arrestins in G protein-coupled receptor regulation. *Annu Rev Pharmacol Toxicol* **38**:289–319.

Lampe M, Pierre F, Al-Sabah S, Krasel C, and Merrifield CJ (2014) Dual single-scission event analysis of constitutive transferrin receptor (TfR) endocytosis and ligand-triggered β2-adrenergic receptor (β2AR) or Mu-opioid receptor (MOR) endocytosis. *Molecular Biology of the Cell* **25**:3070–3080.

Law P-Y, Reggio PH, and Loh HH (2013) Opioid receptors: toward separation of analgesic from undesirable effects. *Trends in Biochemical Sciences* **38**:275–282.

Lee H-J, and Zheng JJ (2010) PDZ domains and their binding partners: structure, specificity, and modification. *Cell Commun Signal* **8**:8.

Lee M-H, Appleton KM, Strungs EG, Kwon JY, Morinelli TA, Peterson YK, Laporte SA, and

Luttrell LM (2016) The conformational signature of β-arrestin2 predicts its trafficking and signalling functions. *Nature* **531**:665–668.

Lefkowitz RJ, Wisler JW, Xiao K, and Thomsen AR (2014) Recent developments in biased agonism. *Current Opinion in Cell Biology* **27**:18–24.

Lin X, Wang Q, Ji J, and Yu L-C (2010) Role of MEK-ERK pathway in morphine-induced conditioned place preference in ventral tegmental area of rats. *J Neurosci Res* **88**:1595–1604.

Liu AP, Aguet F, Danuser G, and Schmid SL (2010) Local clustering of transferrin receptors promotes clathrin-coated pit initiation. *The Journal of Cell Biology* **191**:1381–1393.

Loerke D, Mettlen M, Yarar D, Jaqaman K, Jaqaman H, Danuser G, and Schmid SL (2009) Cargo and dynamin regulate clathrin-coated pit maturation. *PLoS Biol* **7**:e57.

Lohse MJ, Benovic JL, Codina J, Caron MG, and Lefkowitz RJ (1990) beta-Arrestin: a protein that regulates beta-adrenergic receptor function. *Science* **248**:1547–1550.

Luttrell LM, and Lefkowitz RJ (2002) The role of beta-arrestins in the termination and transduction of G-protein-coupled receptor signals. *Journal of Cell Science* **115**:455–465.

Luttrell LM, Ferguson SS, Daaka Y, Miller WE, Maudsley S, Rocca Della GJ, Lin F, Kawakatsu H, Owada K, Luttrell DK, Caron MG, and Lefkowitz RJ (1999) Beta-arrestin-dependent formation of beta2 adrenergic receptor-Src protein kinase complexes. *Science* **283**:655–661.

Luttrell LM, Maudsley S, and Bohn LM (2015) Fulfilling the Promise of "Biased" G

Protein-Coupled Receptor Agonism. *Molecular Pharmacology* **88**:579–588.

Macia E, Ehrlich M, Massol R, Boucrot E, Brunner C, and Kirchhausen T (2006) Dynasore, a Cell-Permeable Inhibitor of Dynamin. *Developmental Cell* **10**:839–850.

Macey TA, Bobeck EN, Hegarty DM, Aicher SA, Ingram SL, and Morgan MM (2009) Extracellular signal-regulated kinase 1/2 activation counteracts morphine tolerance in the periaqueductal gray of the rat. *Journal of Pharmacology and Experimental Therapeutics* **331**:412–418.

Manglik A, Lin H, Aryal DK, McCorvy JD, Dengler D, Corder G, Levit A, Kling RC, Bernat V, Hübner H, Huang XP, Sassano MF, Giguère PM, Löber S, Da Duan, Scherrer G, Kobilka BK, Gmeiner P, Roth BL, Shoichet BK (2016) Structure-based discovery of opioid analgesics with reduced side effects. *Nature* **537**:185-190.

McMahon HT, and Boucrot E (2011) Molecular mechanism and physiological functions of clathrin-mediated endocytosis. *Nat Rev Mol Cell Biol* **12**:517–533.

McPherson J, Rivero G, Baptist M, Llorente J, Al-Sabah S, Krasel C, Dewey WL, Bailey CP, Rosethorne EM, Charlton SJ, Henderson G, Kelly E (2010) μ-opioid receptors: correlation of agonist efficacy for signalling with ability to activate internalization. *Mol Pharmacol.* **78**:756-66.

Merrifield CJ, Perrais D, and Zenisek D (2005) Coupling between Clathrin-Coated-Pit Invagination, Cortactin Recruitment, and Membrane Scission Observed in Live Cells. *Cell* **121**:593–606.

Mettlen M, and Danuser G (2014) Imaging and Modeling the Dynamics of Clathrin-Mediated Endocytosis. *Cold Spring Harbor Perspectives in Biology*, doi: 10.1101/cshperspect.a017038.

Nobles KN, Xiao K, Ahn S, Shukla AK, Lam CM, Rajagopal S, Strachan RT, Huang TY, Bressler EA, Hara MR, Shenoy SK, Gygi SP, Lefkowitz RJ (2011) Distinct phosphorylation sites on the β(2)-adrenergic receptor establish a barcode that encodes differential functions of β-arrestin. Sci Signal. **4**:ra51.

Nuber S, Zabel U, Lorenz K, Nuber A, Milligan G, Tobin AB, Lohse MJ, and Hoffmann C (2016) β-Arrestin biosensors reveal a rapid, receptor-dependent activation/deactivation cycle. *Nature* **531**:661–664.

Paasche JD, Attramadal T, Kristiansen K, Oksvold MP, Johansen HK, Huitfeldt HS, Dahl SG, and Attramadal H (2005) Subtype-specific sorting of the ETA endothelin receptor by a novel endocytic recycling signal for G protein-coupled receptors. *Molecular Pharmacology* **67**:1581–1590.

Pierce KL, Maudsley S, Daaka Y, Luttrell LM, and Lefkowitz RJ (2000) Role of endocytosis in the activation of the extracellular signal-regulated kinase cascade by sequestering and nonsequestering G protein-coupled receptors. *Proceedings of the National Academy of Sciences* **97**:1489–1494.

Pierce KL, Premont RT, Lefkowitz RJ. Seven-transmembrane receptors (2002) *Nat Rev Mol Cell Biol* **3**:639-50.

Premont, R.T., and Gainetdinov, R.R. (2007). Physiological roles of G protein-coupled receptor

kinases and arrestins. *Annu. Rev. Physiol* **69**:511–534.

Puthenveedu MA, and Zastrow von M (2006) Cargo Regulates Clathrin-Coated Pit Dynamics. *Cell* **127**:113–124.

Raehal KM, and Bohn LM (2014) β-arrestins: regulatory role and therapeutic potential in opioid and cannabinoid receptor-mediated analgesia. *Handb Exp Pharmacol* **219**:427–443.

Raehal KM, Schmid CL, Groer CE, and Bohn LM (2011) Functional selectivity at the μ-opioid receptor: implications for understanding opioid analgesia and tolerance. *Pharmacological Reviews* **63**:1001–1019.

Ritter SL, and Hall RA (2009) Fine-tuning of GPCR activity by receptor-interacting proteins. *Nat Rev Mol Cell Biol* **10**:819–830.

Rivero G, Llorente J, McPherson J, Cooke A, Mundell SJ, McArdle CA, Rosethorne EM, Charlton SJ, Krasel C, Bailey CP, Henderson G, and Kelly E (2012) Endomorphin-2: A Biased Agonist at the -Opioid Receptor. *Molecular Pharmacology* **82**:178–188.

Romero G, Zastrow von M, and Friedman PA (2011) Role of PDZ proteins in regulating trafficking, signaling, and function of GPCRs: means, motif, and opportunity. *Adv Pharmacol* **62**:279–314, Elsevier.

Shenoy SK, Lefkowitz RJ (2011) β-Arrestin-mediated receptor trafficking and signal transduction. *Trends Pharmacol Sci* **32**:521-33.

Smith TH, Blume LC, Straiker A, Cox JO, David BG, McVoy JRS, Sayers KW, Poklis JL,

Abdullah RA, Egertová M, Chen C-K, Mackie K, Elphick MR, Howlett AC, and Selley DE (2015) Cannabinoid Receptor-Interacting Protein 1a Modulates CB1 Receptor Signaling and Regulation. *Molecular Pharmacology* **87**:747–765.

Soohoo AL, and Puthenveedu MA (2013) Divergent modes for cargo-mediated control of clathrin-coated pit dynamics. *Molecular Biology of the Cell* **24**:1725–1734.

Sternini C, Spann M, Anton B, Keith DE Jr, Bunnett NW, von Zastrow M, Evans C, Brecha NC (1996) Agonist-selective endocytosis of mu opioid receptor by neurons in vivo. *Proc Natl Acad Sci U S A* **93**:9241-9246.

Strungs, E. G., & Luttrell, L. M. (2014). Arrestin-dependent activation of ERK and Src family kinases. *Handbook of Experimental Pharmacology* **219**:225–257.

Taylor MJ, Perrais D, and Merrifield CJ (2011) A High Precision Survey of the Molecular Dynamics of Mammalian Clathrin-Mediated Endocytosis. *PLoS Biol* **9**:e1000604.

Thompson GL, Kelly E, Christopoulos A, Canals M. (2015) Novel GPCR paradigms at the μ-opioid receptor. *Br J Pharmacol.* **172**:287-96.

Tobin AB, Butcher AJ, and Kong KC (2008) Location, location, location...site-specific GPCR phosphorylation offers a mechanism for cell-type-specific signalling. *Trends in Pharmacological Sciences* **29**:413–420.

Traub LM, and Bonifacino JS (2013) Cargo recognition in clathrin-mediated endocytosis. *Cold Spring Harbor Perspectives in Biology* **5**:a016790–a016790.

Tsvetanova NG, and Zastrow von M (2014) Spatial encoding of cyclic AMP signaling specificity by GPCR endocytosis. *Nat Chem Biol* 1–6.

Urban JD, Clarke WP, Zastrow von M, Nichols DE, Kobilka B, Weinstein H, Javitch JA, Roth BL, Christopoulos A, Sexton PM, Miller KJ, Spedding M, and Mailman RB (2007) Functional selectivity and classical concepts of quantitative pharmacology. *J Pharmacol Exp Ther* **320**:1–13.

Violin JD, Crombie AL, Soergel DG, Lark MW (2014) Biased ligands at G-protein-coupled receptors: promise and progress. *Trends Pharmacol Sci.* **35**:308-16.

Walther C, Caetano FA, Dunn HA, and Ferguson SSG (2015) PDZK1/NHERF3 differentially regulates corticotropin-releasing factor receptor 1 and serotonin 2A receptor signaling and endocytosis. *Cell Signal* **27**:519–531.

Whistler JL, and Zastrow von M (1998) Morphine-activated opioid receptors elude desensitization by beta-arrestin. *Proceedings of the National Academy of Sciences* **95**:9914–9919.

Williams JT, Ingram SL, Henderson G, Chavkin C, von Zastrow M, Schulz S, Koch T, Evans CJ, Christie MJ (2013) Regulation of μ-opioid receptors: desensitization, phosphorylation, internalization, and tolerance. *Pharmacol Rev.* **65**:223-54.

Wolfe BL, and Trejo J (2007) Clathrin-dependent mechanisms of G protein-coupled receptor endocytosis. *Traffic* **8**:462–470.

Xiao K, McClatchy DB, Shukla AK, Zhao Y, Chen M, Shenoy SK, Yates JR, and Lefkowitz RJ (2007) Functional specialization of beta-arrestin interactions revealed by proteomic analysis. *Proceedings of the National Academy of Sciences* **104**:12011–12016.

Yang X, Zheng J, Xiong Y, Shen H, Sun L, Huang Y, Sun C, Li Y, and He J (2010) Beta-2 adrenergic receptor mediated ERK activation is regulated by interaction with MAGI-3. *FEBS Letters* **584**:2207–2212.

Yu Y, Zhang L, Yin X, Sun H, Uhl GR, and Wang JB (1997) Mu opioid receptor phosphorylation, desensitization, and ligand efficacy. *J Biol Chem* **272**:28869–28874.

Zastrow von M, and Kobilka BK (1992) Ligand-regulated internalization and recycling of human beta 2-adrenergic receptors between the plasma membrane and endosomes containing transferrin receptors. *Journal of Biological Chemistry* **267**:3530–3538.

Zindel D, Butcher AJ, Al-Sabah S, Lanzerstorfer P, Weghuber J, Tobin AB, Bünemann M, and Krasel C (2015) Engineered Hyperphosphorylation of the β2-Adrenoceptor Prolongs Arrestin-3 Binding and Induces Arrestin Internalization. *Molecular Pharmacology* **87**:349–362

Zhang L, Loh HH, and Law P-Y (2013) A novel noncanonical signaling pathway for the μ-opioid receptor. *Molecular Pharmacology* **84**:844–853.

Zheng H, Loh HH, and Law P-Y (2008) Beta-arrestin-dependent mu-opioid receptor-activated extracellular signal-regulated kinases (ERKs) Translocate to Nucleus in Contrast to G protein-dependent ERK activation. *Molecular Pharmacology* **73**:178–190.

Zhou L, and Bohn LM (2014) Functional selectivity of GPCR signaling in animals. *Current Opinion in Cell Biology* **27**:102–108.

Molecular Pharmacology Fast Forward. Published on February 2, 2017 as DOI: 10.1124/mol.116.106633
This article has not been copyedited and formatted. The final version may differ from this version.

Footnotes:

This research was supported by grants from the National Institutes of Health - National Institute on Drug Abuse [DA024698], the National Institutes of Health - National Institute of General Medical Sciences [GM117425], and the National Science Foundation [117776] to MAP. ZYW was partially supported by the National Institutes of Health - National Institute of Neurological Disorders and Stroke [T32 NS007433], and DJS was partially supported by a DeVries Fellowship to Carnegie Mellon University.

Molecular Pharmacology Fast Forward. Published on February 2, 2017 as DOI: 10.1124/mol.116.106633
This article has not been copyedited and formatted. The final version may differ from this version.

Figure Legends

Figure 1: Morphine and Endomorphin-2 have distinct arrestin signaling profiles at WT μR. A) Example montage of nuclear EKAR response in WT μR-expressing cell in response to EM2. Top row: FLAG-tagged μR labeled with Alexa647-conjugated M1 Antibody. Bottom row: ratio of FRET/CFP fluorescence of expressed nEKAR sensor. Agonist added at 5 minutes. Scale bar is 10μM, frames every 3 minutes. B) Representative montage of nEKAR response measured in WT μR-expressing cell in response to morphine. C) Representative traces of nEKAR FRET/CFP ratio for cells treated with either morphine or EM2. A higher amplitude and narrower peak is observed for EM2 compared to morphine. D) EM2 induces a significantly greater peak amplitude compared to morphine (n=33 & 25 respectively, ** $p < 0.01$). E) EM2 produces overall greater ERK response compared to morphine, using area under the curve after agonist treatment to assay total ERK response (n=33 & 25, *$p < 0.0253$). F) Knockdown of β-arrestin1/2 significantly decreases peak ERK response for EM2-treated cells (n=24 & 10 for control and KD respectively, ** $p < 0.01$) but did not significantly change peak for morphine-treated cells (n=12 & 7, n.s.). Insert Fi shows knockdown confirmation, with intense bands from stain-free total protein of the same gel as control. G) Example montage for cEKAR sensor response to EM2, presented in the same manner as A. H) Representative montage of cEKAR response to morphine. I) Representative traces for cytosolic ERK activation for morphine and EM2. J) EM2-dependent peak cytosolic ERK response is significantly higher than morphine (n= 53 & 12, *$p < 0.0253$). K) Total ERK response for EM2 is greater in the cytosol compared to morphine (n = 53 & 12, **$p < 0.01$). L) β-arrestin1/2 knockdown again significantly decreases peak ERK signal for EM2 (n = 29 & 10, *$p < 0.05$) while having no effect on morphine peak response (n=12 & 6, n.s.).

Molecular Pharmacology Fast Forward. Published on February 2, 2017 as DOI: 10.1124/mol.116.106633
This article has not been copyedited and formatted. The final version may differ from this version.

Figure 2: Arrestin colocalizes with μR clusters for the duration of their endocytic lifetime.

A) Representative montage showing the recruitment timing and colocalization duration for β-arrestin2 with μR in response to EM2. Top row in montage is an Alexa-647 labeled FLAG-μR, middle row is a GFP-tagged β-arrestin2. Simultaneous fluorescence increases in both channels is seen as well as simultaneous rapid disappearance. B) Representative montage for arrestin and receptor colocalization after treatment with morphine. C) Cells expressing WT FLAG-μR and arrestin (shown) before and after morphine treatment. Notable clustering is seen arrestin channel rapidly after agonist addition (see arrow in middle column merge) and clusters rapidly disappear with new clusters forming (see difference in identified objects between middle and last columns) Scale bar is 5μM. D) Arrestin vs. μR fluorescence for tracks across a variety of lifetime cohorts. Clusters analyzed with cmeAnalysis were grouped into 4 lifetime cohorts (0-77s n = 1600 clusters, 80-157s n = 141, 160-237s n = 16, 241-320s, n = 2). Arrestin intensity at clusters roughly overlaps with receptor fluorescence. E) Overall population lifetimes of arrestin cluster lifetimes performed through manual quantification. There is higher max and median cluster lifetimes seen for EM2 compared to morphine. (n = 149 & 73 clusters for EM2 and morphine respectively). F) Mean lifetime of arrestin clusters. EM2 induces a significantly higher mean lifetimes of arrestin clusters compared to morphine (n = 149 & 73 clusters respectively, ***$p < 0.001$). G) Automated quantification of the same movies used for E & F performed with cmeAnalysis package. The number of clusters with lifetimes greater than 150s are displayed here as a fraction of total clusters detected per cell ± SEM (3 cells for EM2, 7 cells for morphine, total n = 19549 & 21665 for clusters in respective conditions). H) Empirical distribution functions for

observed lifetimes over 150s. Curves originate from distinct cumulative distributions as confirmed by Kolmogorov-Smirnov test (D = 0.333, ***p < 0.001).

Figure 3: Mutation of a bi-leucine sequence in μR C-terminus decreases EM2-dependent lifetimes of arrestin clusters but does not affect arrestin recruitment kinetics. A) Population lifetime distributions for arrestin clusters measured after EM2 addition for WT or LLAA μR (n = 152 & 151 clusters, respectively). B) Mean lifetimes for arrestin clusters with either WT or LLAA μR. LLAA μR induced significantly shorter overall mean lifetime for arrestin (*** p < 0.001). C) Automated quantification was conducted on the same movies analyzed for A and B using cmeAnalysis. The number of clusters with lifetimes greater than 150s are displayed here as a fraction of total clusters detected per cell ± SEM (3 cells for WT μR, 3 cells for LLAA μR, total n = 19549 & 26647 for clusters in respective conditions). D) Empirical distribution functions for both populations. Curves originate from distinct cumulative distributions as confirmed by Kolmogorov-Smirnov test (D = 0.5854, ***p < 0.001). E) Global arrestin recruitment in cells expressing WT μR (top row) or LLAA μR (bottom row) following EM2 (10μM) treatment. Cells expressing tdTomato-tagged β-arrestin2 were imaged after agonist treatment at 10hz. Formation of initial diffraction limited clusters can be seen in both cell lines within 10s, with maximal clustering visible within 50s after agonist treatment. F) Individual arrestin cluster recruitment kinetics were measured using high speed (10hz) imaging. Clusters were analyzed with cmeAnalysis, and then individual cluster fluorescence was normalized from min-to-max. Graph shows normalized cluster fluorescence over time (n = 482 clusters for WT, 982 clusters for LLAA), with dashed lines representing 95% CI.

Molecular Pharmacology Fast Forward. Published on February 2, 2017 as DOI: 10.1124/mol.116.106633
This article has not been copyedited and formatted. The final version may differ from this version.

Figure 4: LLAA μR has diminished ERK activation compared to WT μR, but is equally capable of activating G-protein dependent signaling. A) Peak nuclear ERK response as measured by EKAR is much greater for WT μR compared to LLAA μR when both are stimulated by EM2 (n = 33 & 22 for WT and LLAA μR respectively, ***$p < 0.001$). B) Total ERK response is diminished for LLAA μR compared to WT in the nucleus (n = 33 & 22 for WT and LLAA μR, ***$p < 0.001$). C) The same pattern is seen in the cytosol, with WT μR eliciting a greater peak response compared to the mutant receptor (n = 53 & 40, *$p < 0.0253$) and D) a higher total ERK response as measured by AUC (n = 53 & 40, **$p < 0.001$). E) Difference in total ERK response following agonist treatment is dependent on agonist ability to recruit arrestin as described in McPherson *et al.,* 2010. Agonists were all used at 10μM, all reported measurements were collected using cEKAR as output for ERK signaling. Mean AUC after treatment for LLAA was subtracted from mean AUC from the same agonist for WT μR, difference scores are reported here. Error bars represent 95% confidence intervals on difference score (n = 11 & 10 for fentanyl WT & LLAA respectively, n = 9 & 8 for methadone, 6 & 8 for DAMGO, 11 & 4 for morphine, 53 & 40 for EM2, and 34 & 38 for oxycodone). F) Example montage of cAMP sensor EPAC in WT μR-expressing cells. From left to right, images show time course for the same cell, each taken 5 minutes apart. Forskolin is added at 5 minutes to stimulate cAMP production, EM2 added at 10 minutes. Top row: Alexa647-labeled μR. Bottom row: FRET ratio presented as CFP/FRET fluorescence. Scale bar is 10μm. G) Example montage of EM2 ability to inhibit cAMP production in LLAA μR-expressing cells. H) Example traces from WT μR or LLAA μR-expressing cells treated with either forskolin followed by EM2, or

forskolin alone. I) Percentage decrease in cAMP production during treatment window, measured as average FRET ratio during forskolin treatment (5-10 minutes) minus average ratio during manipulation (EM2 or no additional treatment, 10-15 minutes) divided by max response minus baseline (0-5 minutes) A main effect of treatment was seen by oneway ANOVA (*** $p < 0.001$) with Bonferroni post-hoc showing no difference between WT and LLAA conditions, but both being significantly different from FSK-only (* $p < 0.05$).

Figure 5: Extension of endocytic cluster lifetimes with dynasore enhances EM2 signaling at LLAA μR and morphine signaling at WT μR. A) Kymograph showing lifetimes of LLAA μR clusters (time on X axis). Each pixel column represents one frame, frames taken every 3s. EM2 added at 1 minute, then imaged for 10 minutes. Left image show cells pretreated with DMSO. Right image, cells were pretreated with 40μM dynasore for 20 minutes before imaging, and dynasore was left in the imaging media to maintain endocytosis suppression. B) Boxplot showing difference in population lifetimes in response to dynasore pretreatment ($n = 33$ & 32 clusters for EM2 and EM2 + Dynasore respectively, *** $p < 0.001$). C) Representative immunoblot for phospho-ERK1/2 in cells expressing LLAA μR and treated with EM2 for 5 minutes and pretreated for 20 minutes with either 40μM dynasore or DMSO. Top row is phospho-ERK (Thr202), bottom row is ERK1/2 as loading control. D) Quantification of 7 separate blots with no treatment response normalized to 1 for each blot. Dynasore pretreatment increases EM2-dependent ERK response. A significant effect of treatment was seen via a repeated-measures oneway ANOVA (* $p < 0.05$), with a significant difference seen in post-hoc comparison of dynasore-treated vs DMSO-treated in the presence of EM2. (E) Representative

immunoblot of WT μR-expressing cells pretreated with either dynasore 40μM or DMSO and then treated with morphine 5 or 10. F) Quantification of 8 separate blots. Dynasore pretreatment increases total ERK response at 5 minutes. A significant effect of treatment was seen via a repeated-measures oneway ANOVA (* $p < 0.05$), with a significant difference seen in post-hoc comparison of dynasore-treated vs DMSO-treated in the presence of morphine.

Figure 1

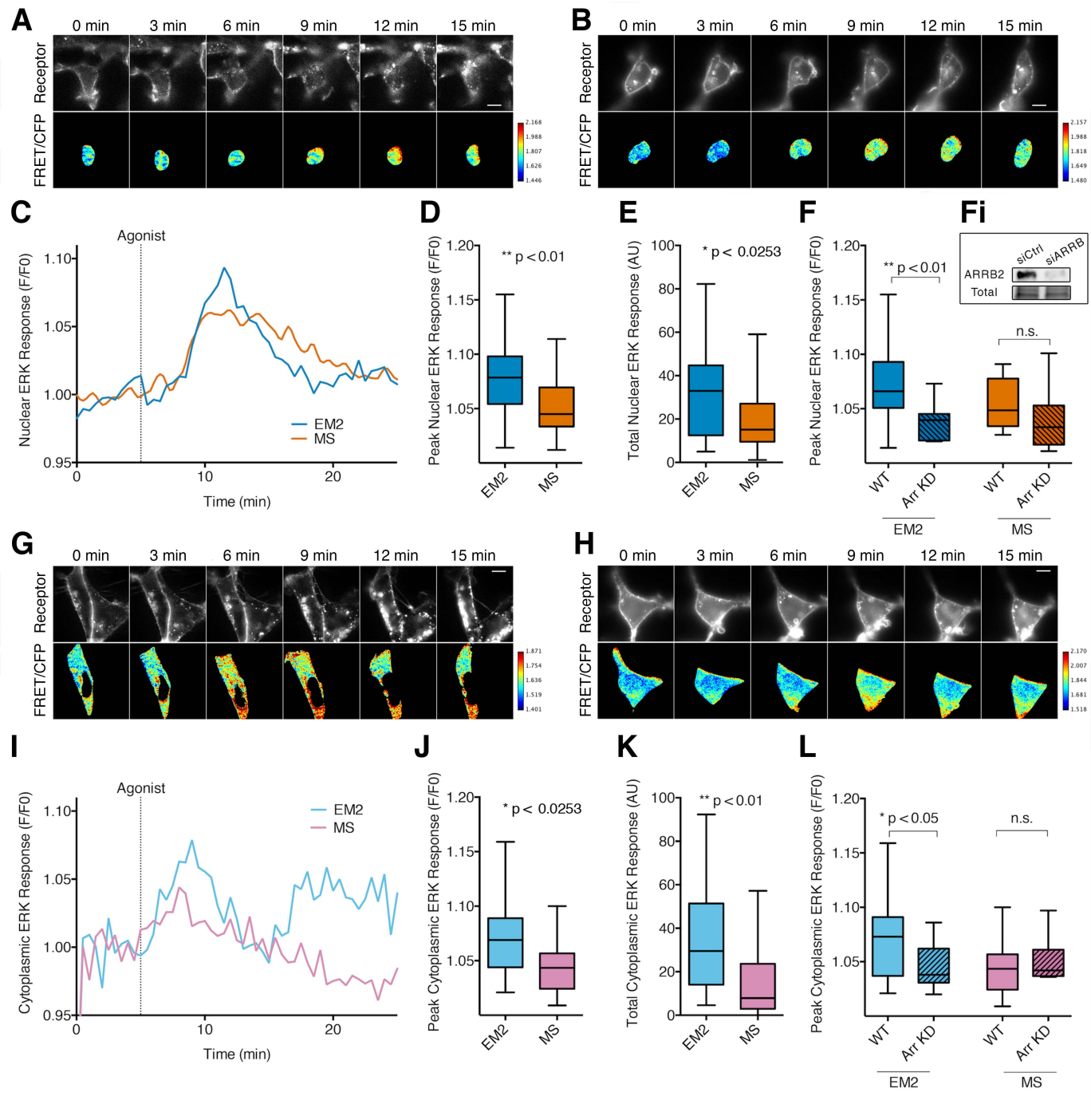
A
0 min
3 min
6 min
9 min
12 min
15 min
Receptor
FRET/CFP
2.168
1.988
1.807
1.626
1.446
B
0 min
3 min
6 min
9 min
12 min
15 min
Receptor
FRET/CFP
2.157
1.988
1.818
1.649
1.480
C
Agonist
Nuclear ERK Response (F/F0)
1.10
1.05
1.00
0.95
0
10
20
Time (min)
EM2
MS
D
Peak Nuclear ERK Response (F/F0)
** p < 0.01
1.20
1.15
1.10
1.05
EM2
MS
E
Total Nuclear ERK Response (AU)
* p < 0.0253
100
80
60
40
20
0
EM2
MS
F
Peak Nuclear ERK Response (F/F0)
** p < 0.01
n.s.
1.20
1.15
1.10
1.05
WT
Arr KD
WT
Arr KD
EM2
MS
Fi
siCtrl
siARRB
ARRB2
Total
G
0 min
3 min
6 min
9 min
12 min
15 min
Receptor
FRET/CFP
1.871
1.754
1.636
1.519
1.401
H
0 min
3 min
6 min
9 min
12 min
15 min
Receptor
FRET/CFP
2.170
2.007
1.844
1.681
1.518
I
Agonist
Cytoplasmic ERK Response (F/F0)
1.10
1.05
1.00
0.95
0
10
20
Time (min)
EM2
MS
J
Peak Cytoplasmic ERK Response (F/F0)
* p < 0.0253
1.20
1.15
1.10
1.05
EM2
MS
K
Total Cytoplasmic ERK Response (AU)
** p < 0.01
100
80
60
40
20
0
EM2
MS
L
Peak Cytoplasmic ERK Response (F/F0)
* p < 0.05
n.s.
1.20
1.15
1.10
1.05
WT
Arr KD
WT
Arr KD
EM2
MS

Figure 2

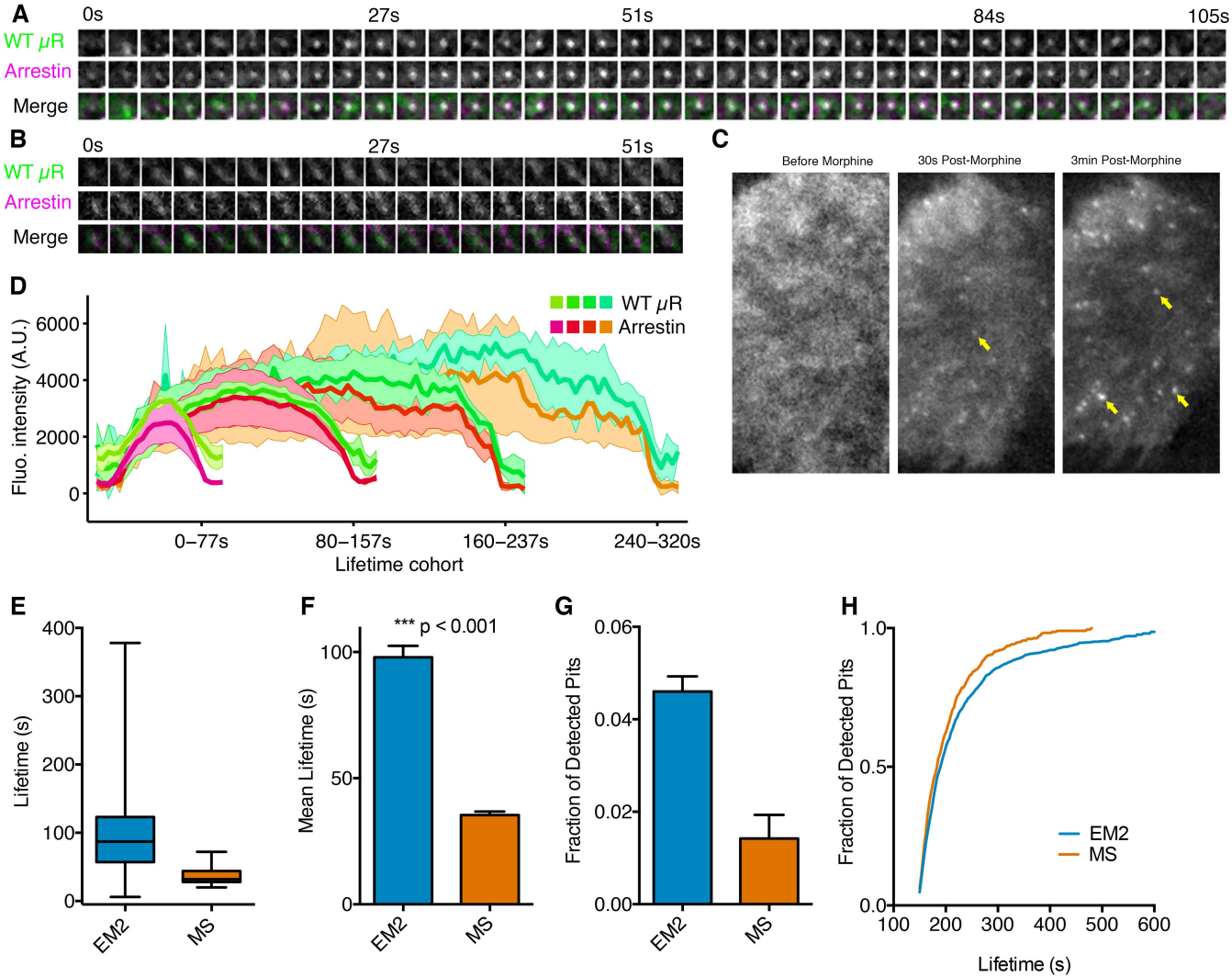
A
0s
27s
51s
84s
105s
WT μR
Arrestin
Merge
B
0s
27s
51s
WT μR
Arrestin
Merge
C
Before Morphine
30s Post-Morphine
3min Post-Morphine
D
WT μR
Arrestin
Fluo. intensity (A.U.)
6000
4000
2000
0
0–77s
80–157s
160–237s
240–320s
Lifetime cohort
E
Lifetime (s)
400
300
200
100
0
EM2
MS
F
*** p < 0.001
Mean Lifetime (s)
100
50
0
EM2
MS
G
Fraction of Detected Pits
0.06
0.04
0.02
0.00
EM2
MS
H
Fraction of Detected Pits
1.0
0.5
0.0
EM2
MS
100
200
300
400
500
600
Lifetime (s)

Figure 3

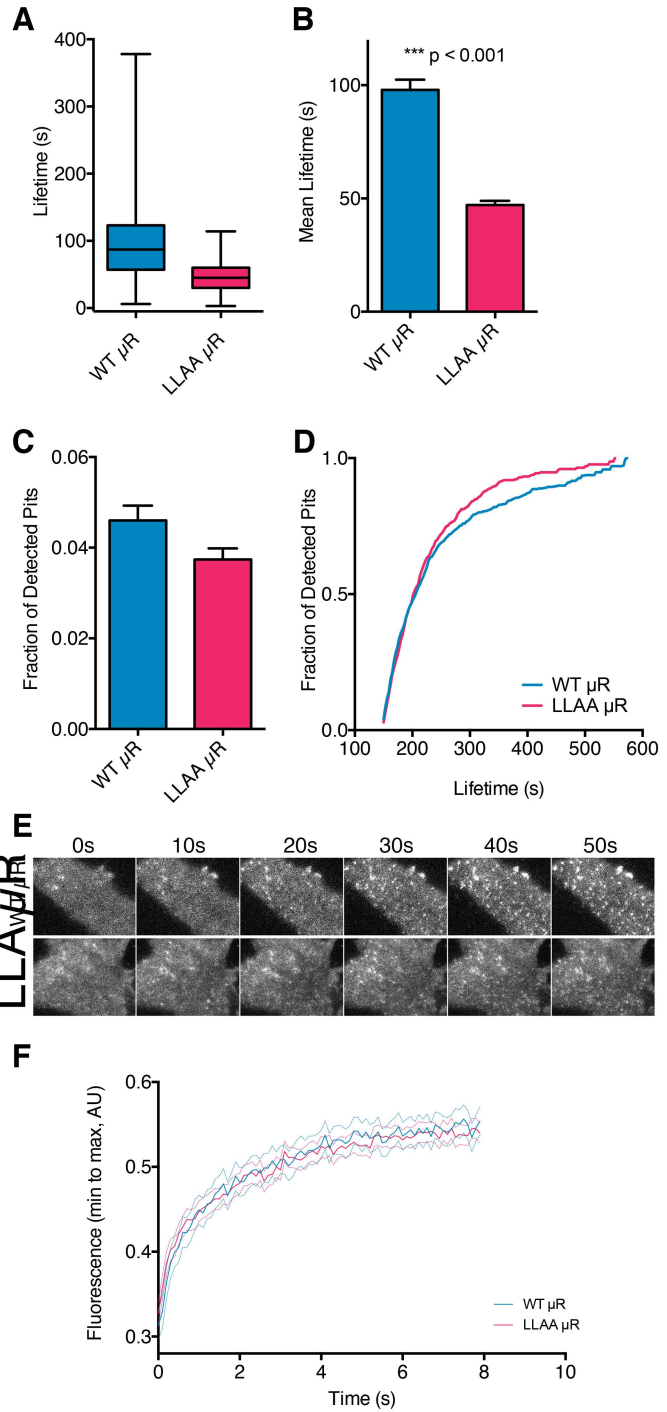
A
Lifetime (s)
400
300
200
100
0
WT μR
LLAA μR
B
*** p < 0.001
Mean Lifetime (s)
100
50
0
WT μR
LLAA μR
C
Fraction of Detected Pits
0.06
0.04
0.02
0.00
WT μR
LLAA μR
D
Fraction of Detected Pits
1.0
0.5
0.0
100
200
300
400
500
600
Lifetime (s)
WT μR
LLAA μR
E
0s
10s
20s
30s
40s
50s
WT μR
LLAA μR
F
Fluorescence (min to max, AU)
0.6
0.5
0.4
0.3
0
2
4
6
8
10
Time (s)
WT μR
LLAA μR

Figure 4

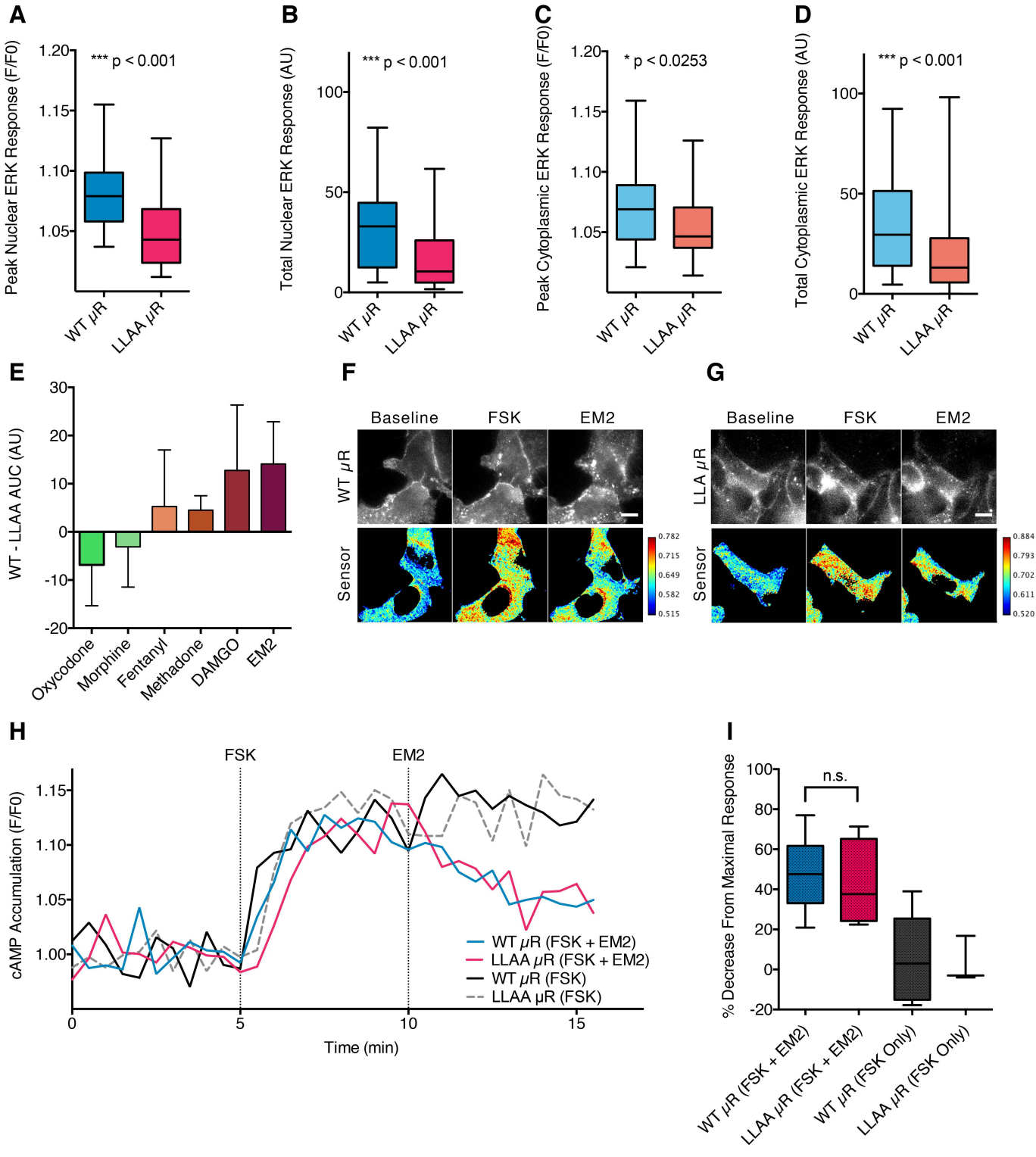
A
Peak Nuclear ERK Response (F/F0)
*** p < 0.001
WT μR
LLAA μR
B
Total Nuclear ERK Response (AU)
*** p < 0.001
C
Peak Cytoplasmic ERK Response (F/F0)
* p < 0.0253
D
Total Cytoplasmic ERK Response (AU)
*** p < 0.001
E
WT - LLAA AUC (AU)
Oxycodone
Morphine
Fentanyl
Methadone
DAMGO
EM2
F
Baseline
FSK
EM2
WT μR
Sensor
G
LLA μR
H
cAMP Accumulation (F/F0)
FSK
EM2
WT μR (FSK + EM2)
LLAA μR (FSK + EM2)
WT μR (FSK)
LLAA μR (FSK)
Time (min)
I
% Decrease From Maximal Response
n.s.
WT μR (FSK + EM2)
LLAA μR (FSK + EM2)
WT μR (FSK Only)
LLAA μR (FSK Only)

Figure 5

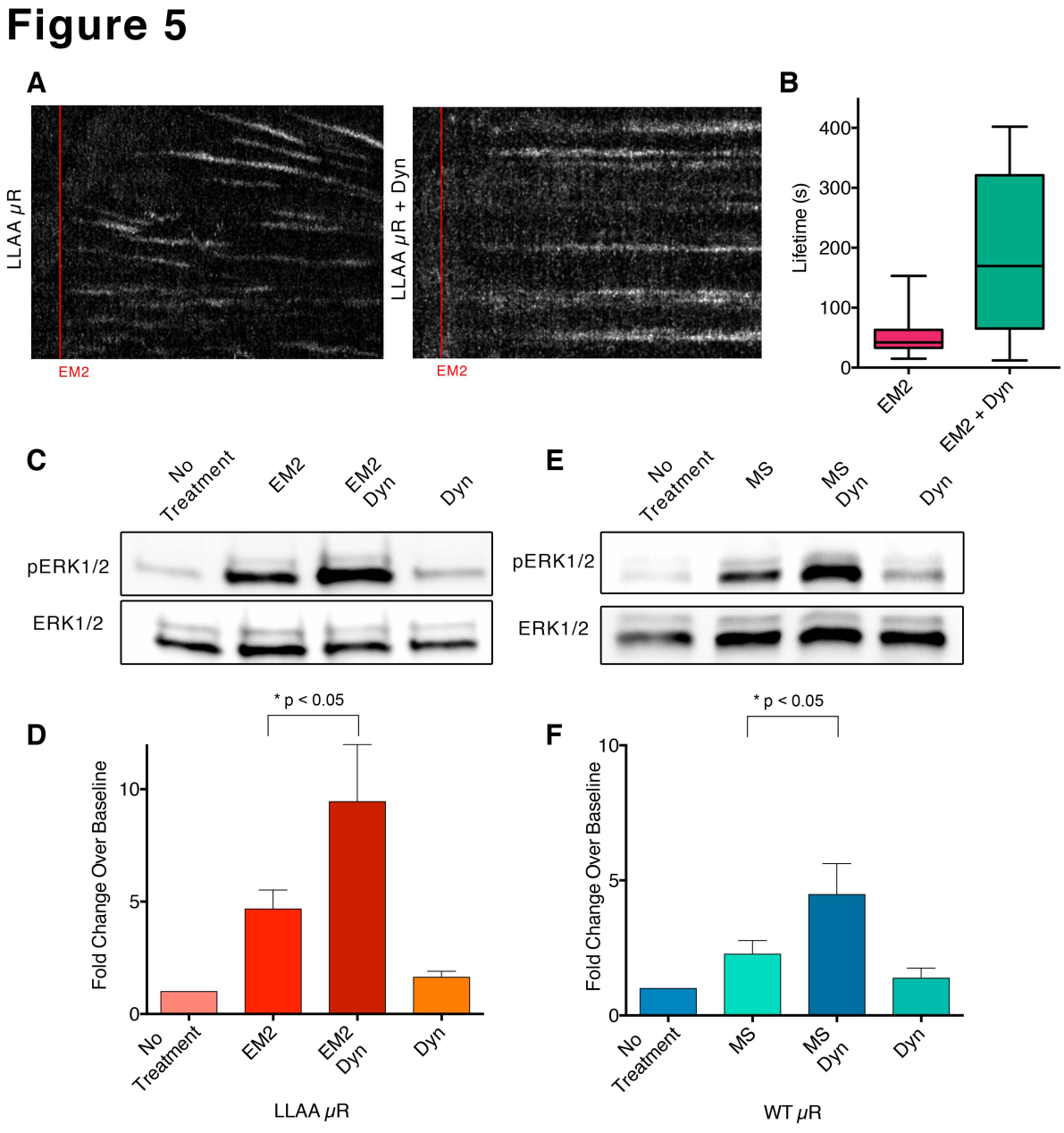
A
LLAA μR
EM2
LLAA μR + Dyn
EM2
B
Lifetime (s)
400
300
200
100
0
EM2
EM2 + Dyn
C
No Treatment
EM2
EM2 Dyn
Dyn
pERK1/2
ERK1/2
E
No Treatment
MS
MS Dyn
Dyn
pERK1/2
ERK1/2
D
* p < 0.05
Fold Change Over Baseline
10
5
0
No Treatment
EM2
EM2 Dyn
Dyn
LLAA μR
F
* p < 0.05
Fold Change Over Baseline
10
5
0
No Treatment
MS
MS Dyn
Dyn
WT μR